Applied Water Science (2023) 13:144
https://doi.org/10.1007/s13201-023-01948-9

ORIGINAL ARTICLE

Smart guanyl thiosemicarbazide functionalized dialdehyde cellulose for removal of heavy metal ions from aquatic solutions: adsorption characteristics and mechanism study

Magda A. Akl[1] · **Abdelrahman S. El-Zeny**[1] · **Mohamed Ismail**[1,1] · **Mohamed Abdalla**[1,1] · **Dina Abdelgelil**[1] · **Aya G. Mostafa**[1]

Received: 6 March 2023 / Accepted: 15 May 2023 / Published online: 3 June 2023
© The Author(s) 2023

Abstract

In recent years, facing the problem of improving environmental quality, cellulose and cellulose-based (nano) composites have received great attention as adsorbents. In this work, we report the modification and functionalization of cellulose by nitrogen- and sulfur-containing moieties through a three-steps process; native cellulose is first oxidized by potassium periodate (KIO_4) to form dialdehyde cellulose (DAC), which then condenses with aminoguanidine and react with phenyl isothiocyanate to form 4-phenyl guanyl thiosemicarbazide dialdehyde cellulose (DAC@GuTSC). The prepared DAC@GuTSC is characterized by a number of techniques, including Fourier transform infrared spectroscopy (FTIR), scanning electron microscopy (SEM), elemental analysis (EA), Brunauer–Emmett–Teller (BET) and thermogravimetric analysis (TGA). The prepared DAC@GuTSC adsorbent was used to remove Cu^{2+} Hg^{2+} and Pb^{2+} from aqueous solution and environmental water samples. The influence of various factors on the adsorption efficiency including pH, initial metal concentration, contact time, adsorbent dosage, temperature, and ions interfering with adsorption was investigated. Under optimal adsorption conditions, the adsorption capacity of Cu^{2+}, Hg^{2+} and Pb^{2+} was 50, 94 and 55 mg g^{-1}, respectively. The adsorption process is well described by the Langmuir model, and it was found to follow the pseudo-second-order kinetics model. The spontaneous and endothermic adsorption of Cu^{2+}, Hg^{2+} and Pb^{2+} was confirmed by the calculated thermodynamic functions. The prepared DAC@GuTSC composite has been successfully applied to remove Cu^{2+}, Hg^{2+} and Pb^{2+} from real water samples with recovery greater than 90% and relative standard deviation (RSD) less than 3%. The reasonable Cu^{2+}, Hg^{2+} and Pb^{2+}adsorption mechanism on the prepared DAC@GuTSC composite has been elucidated.

Keywords Adsorption · Cellulose · Aminoguanidine · Phenyl isothiocyanate · Heavy metals · Water treatment

Introduction

Clean and safe water is an eternal need of every individual. In recent decades, freshwater resources have been directly threatened by increasing industrialization worldwide (Jamil et al. 2009).Discharged industrial waste significantly contaminates water sources by releasing a number of pollutants, including organics and heavy metals (Liu and Huang 2011). Unlike organic pollutants, heavy metals such as Hg, Pb, Cu, Cd and Zn are not biodegradable and tend to accumulate and persist for long periods (Nouri et al. 2007). These heavy metals can cause a number of diseases and disorders, even at very small concentrations (Gotoh et al. 2004a, 2004b). For example, lead has a number of health effects, including anemia, hypertension and digestive disorders (Gherasim and Mikulášek 2014; Martin and Griswold 2009) while high copper levels can cause abdominal strain and kidney failure (Bilal et al. 2013; Chaturvedi 2013) mercury is believed to have toxic effects on the nervous system, leading to serious disorders such as brain damage, memory loss, behavioral abnormalities and autism (Chang 1977; Clarkson 1993; Clarkson and Magos 2006; Friberg and Mottet 1989; Guzzi and La Porta 2008; Magos and Clarkson 2006).

To avoid serious impacts on the environment and public health, several techniques have been developed to remove heavy metals from water, including ion exchange, chemical

✉ Magda A. Akl
magdaakl@yahoo.com

[1] Department of Chemistry, Faculty of Science, Mansoura University, Mansoura 35516, Egypt

precipitation, membrane filtration and adsorption. (Akl et al. 2013, 2005, 2004; Atta et al. 2013; Ibrahim et al. 2019; Kurniawan et al. 2006; Lee et al. 2007; Meena et al. 2005; Monier et al. 2014b, 2014a; Nayl et al. 2020; O'Connell et al. 2008; Shoueir et al. 2016, 2017; Wang and Li 2013; Zewail and Yousef 2015). However, adsorption is widely preferred over other conventional techniques due to its affordability, simplicity, high efficiency and eco-friendly nature (Aydın et al. 2008; Hua et al. 2012; Khan et al. 2004; Pan et al. 2009; Zhao et al. 2010).

Cellulose is one of the most commonly used biosorbents, showing great heavy metal adsorption potential, especially when chemically modified by binding to novel groups via complexation or chelation significantly improves its adsorption capacity (Acemioglu and Alma 2001; Aydın et al. 2008; Dridi-Dhaouadi et al. 2011; Gupta 2009; Navarro et al. 1996; Suhas et al. 2016; Wu et al. 2012). It has been shown that introducing aminoguanidine to cellulose after oxidizing it with KIO_4 improves its adsorption capacity and leads to satisfactory removal results for Cu ions, Hg, Pb, Cd and Zn of aqueous solutions (Kenawy et al. 2018).

In this study, an attempt was made to modify cellulose by adding an additional procedure to the above method, that is, adding phenyl isothiocyanate to aminoguanidine modified cellulose and investigating its effectiveness in adsorbing three heavy metals (i.e., Cu, Hg and Pb) from aqueous solution and real sample. This modification leads to the formation of a new adsorbent 4-pheny guanyl thiosemicarbazide functionalized dialdehyde cellulose (DAC@GuTSC) containing potentially electron-donating N and S atoms. The presence of N/S atoms provides a stronger chelation regime with metal ions.

To our knowledge, the modification of cellulose using a nitrogen-containing ligand (aminoguanidine) and a sulfur-nitrogen phenyl isothiocyanate has not been reported in the literature. Again, no data were found on using DAC@GuTSC modified cellulose as an effective adsorbent for Cu^{2+}, Hg^{2+} and Pb^{2+} from actual polluted water samples.

Accordingly, the current study was performed out with these objectives:

i. Design and synthesis of N and S containing guanyl thiosemicarbazide functionalized dialdehyde cellulosic composite (DAC@GuTSC) for adsorption of Cu^{+2}, Hg^{+2} and Pb^{+2} metal ions in single and multi-component metal ions' solutions.
ii. Characterization of the as-prepared DAC@GuTSC composite using physical (optical images) elemental analysis and spectroscopic (FTIR), SEM and TGA instrumental performances.
iii. Batch sorption experiments in single and multi-component metal ions utilizing Cu^{2+}, Hg^{2+} and Pb^{2+}as pollutants.

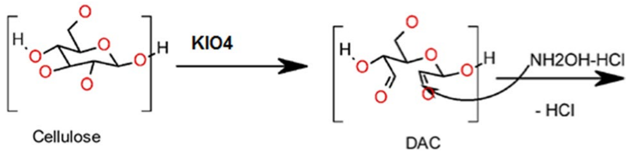

Scheme 1 Schematic representation of determination of the aldehyde content (Dacrory 2021)

iv. Investigating the ideal parameters required for optimal adsorption of the studied metal ions, e.g., pH, temperature, the initial concentration of the three investigated metal ions, the mass of DAC@GuTSC composite and the oscillation time, as well as the interfering ions.
v. Studying the various adsorption isotherm, kinetics and thermodynamic parameters.
vi. Comparative evaluation of metal removal efficiency and reusability of DAC@GuTSC composite with other previously reported adsorbents.
vii. Elucidation of the mechanisms involved in the process of adsorption of Cu^{+2}, Hg^{+2} and Pb^{+2} onto DAC@GuTSC composite.

Experimental and methods

Materials

Aminoguanidine monohydrochloride, cellulose powder, phenyl isothiocyanate, potassium metaperiodate (KIO_4), $CuSO_4$, $HgCl_2$, $Pb(NO_3)_2$ and triethylamine were purchased from Sigma-Aldrich and directly used.

Preparations

Preparation of dialdehyde cellulose (DAC)

One gram of the native cellulose was oxidized using 100 ml of 4% potassium periodate. The previous mixture was shaken for 1 h in complete darkness to form dialdehyde cellulose (DAC), Scheme 1. The obtained DAC was washed several times with dist.H_2O and was dried in an oven at 50 °C.

Determination of aldehyde content The aldehyde content of DAC is determined by the Schiff base reaction in Fig. 1 according to refs (Dacrory 2021; Dacrory et al. 2019) in which hydroxylamine hydrochloride is used to convert the aldehyde group to the corresponding oxime. 0.3 g of DAC sample was dispersed in 20 ml of distilled water and adjusted to ($pH \approx 5$) with NAOH solution. 20 ml of hydroxylamine hydrochloride solution (0.72 mol/l) of pH 5 was then added. The mixture was stirred at 40 °C for

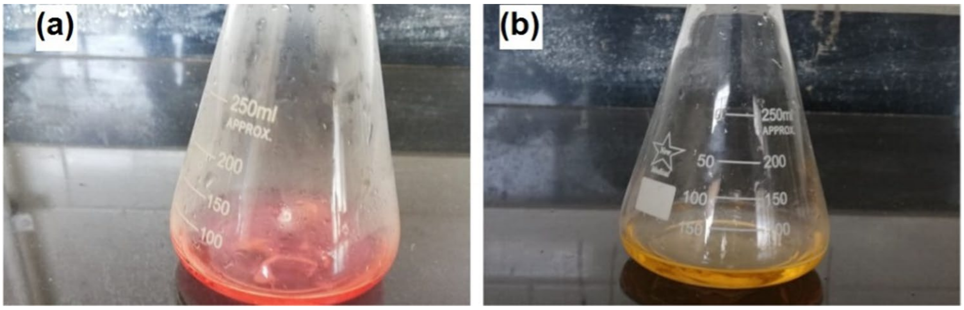

Fig. 1 **a** Filtrate of 0.25 M hydroxylamine after stirring for 2.5 h with DAC; **b** after titration with 0.1 M NaOH

4 h. Released HCl was titrated with 1.0 M NaOH solution. The amount of NaOH consumed when the pH of the solution reached 5.0 was recorded (Ibrahim et al. 2019). The amount of NaOH solution consumed in the titration was recorded as Va (liters). A pH 5.0 cellulose solution of the same concentration was used as a blank and the volume of 1.0 M NaOH consumed was recorded as Vc (liters). Aldehyde content (% w/w) calculated using the following formula (Dacrory 2021)

$$-\mathrm{CHO} + \mathrm{NH_2OH} - \mathrm{HCl} \rightarrow -\mathrm{CHNOH} + \mathrm{HCl} + \mathrm{H_2O}$$

$$\mathrm{HCl} + \mathrm{NaOH} \rightarrow \mathrm{NaCl} + \mathrm{H_2O}$$

The aldehyde content for DAC was calculated as shown in Eq. 1:

$$\mathrm{AC}(\%) = \frac{M_{\mathrm{NaOH}}\left(V_{\mathrm{sample}} - V_{\mathrm{control}}\right)}{{}^{m}/_{Mwt}} \times 100 \tag{1}$$

Where M_{NaOH} is the used NaOH concentration (0.1 mol), m is the prepared DAC weight, and Mwt is the molecular weight of the DAC repeating unit $(C_6H_8O_{10})_n$ that is equal to 160.124 g/mol. V_{sample} and V_{control} are the recorded volumes of the NaOH consumption for the DAC sample and control one, respectively. The determination of the aldehyde content for DAC is schematically represented in scheme 1

Preparation of the Schiff base guanyl thiosemicarbazide functionalized dialdehyde cellulose (DAC@GuTSC)

Guanyl dialdehyde cellulose (DAC@Gu) was prepared by the same procedure followed in the mentioned study [45] except for increasing the oxidation time for 6 h. Then, 5 ml of phenyl isothiocyanate was added to 0.5 g of the guanyl modified cellulose and immersed in 100 ml of ethanol in the presence of triethylamine. The obtained mixture was allowed to reflux for 3 h at 80 °C. Yellow powder of the guanyl 4-phenyl thiosemicarbazide functionalized dialdehyde cellulose composite (DAC@GuTSC) was obtained at the end.

Instrumentation

The FTIR spectra of the prepared samples were recorded between 4000 and 400 cm^{-1}. Disks were prepared by first mixing 1 mg of dried samples with 500 mg of KBr (Merck, for spectroscopy) in an agate mortar and then pressing the resulting mixture successively at 8 tons cm^{-2}. Elemental analysis was done using a Perkin-Elmer 2400 analyzer. Brunauer–Emmett–Teller (BET) analysis was conducted to evaluate the surface area of the DAC@GuTSC. Thermogravimetric analysis (TGA) was performed by thermo analyzer Shimatzu DT40 (Japan) over temperature range of 30–800 °C with N_2 atmosphere and with the heating flow 10 °C/min. In addition, scanning electron microscope (SEM) was used to study the morphology of native cellulose, DAC and DAC@GuTSC samples. The samples were sputtered and coated with gold before using scanning electron microscope. The concentrations of Cu^{2+}, Hg^{2+} and Pb^{2+} in metal solutions before and after adsorption were estimated using Agilent's 5100 ICP OES.

The point of zero charge (pH_{PZC}) was determined using the solid addition method. In a series of 100 ml jacketed glasses, 50 ml of KNO_3 solutions of known concentration was transferred. The solutions of different initial pH (pH_i) between 2 and 12 were prepared by adding either 0.1 M HCl or 0.1 M NaOH. One gram of DAC@GuTSC composite was then added to each solution with stirring for 48 h. The final pH (pH_f) was measured and the difference between the initial and final pH values ($\Delta pH = pH_i$- pH_f) was plotted against pHi. The pHpzc value is the point where the curve ΔpH vs pHi crosses the line $\Delta pH = 0$.

Batch adsorption experiments

Batch adsorption of Cu^{2+}, Hg^{2+} and Pb^{2+} was performed in 100 mL reagent bottles containing 50 mL of known initial concentrations (50, 100, 150, 200) ppm of the metals under investigation and known DAC@GuTSC weights (0.01, 0.03, 0.05) g at a pH of (3–7) adjusted by the addition of 0.1 M NaOH and/or 0.1 M HCL and a temperature of (25–45)°C (at time intervals of 1–24 h). Bottles containing samples were shaken on a mechanical shaker for (20–120 min) and filtered. Metal ion concentrations in the supernatants were determined by ICP OES.

Then, adsorption capacity and the removal efficiency were evaluated by Eqs. (2) and (3), respectively.

$$q_e = \left(C_i - C_e\right)V/W \tag{2}$$

$$\text{Removal (\%)} = \frac{\left(C_i - C_e\right)}{C_i} \times 100 \tag{3}$$

where q_e is the adsorption capacity in mg g^{-1}, C_i is the initial concentration of metal ion under study in (mg L^{-1}), C_e is the equilibrium concentration of metal ions in (mg L^{-1}), V volume of solution in (liter), and W is adsorbent mass in (g).

Results and discussion

Materials' design

Synthesis of dialdehyde cellulose (DAC)

KIO_4, a known selective oxidizing agent, oxidizes two hydroxyl groups on two neighboring carbon atoms C_2–C_3 bond of the glucopyranoside ring that will be cleaved and converted into two dialdehyde groups. The oxidation degree which represents the percentage of monosaccharide units that reacted with KIO_4 is calculated by aldehyde content determination (Akl et al. 2021). The aldehyde content of the prepared DAC is 35.71% as it is presented in Table1.

Synthesis of the Schiff base DAC@GuTSC composite

Natural cellulose powder was selectively oxidized by KIO_4 to give the dialdehyde form (DAC) with aminoguanidine at 80 °C. The product (DAC@Gu) was further reacted with phenyl isothiocyanate to form the DAC@GuTSC composite with additional nitrogen and sulfur functionalities. The water solubility of the DAC@GuTSC adsorbent was tested by suspending a 1.00 g sample of the DAC@GuTSC adsorbent in 50.0 mL of water. After stirring the suspension for about 3.0 h, the resulting solid was collected by filtration and dried. No reduction in total mass was observed. The DAC@GuTSC adsorbent was insoluble in water. Scheme 2 represents the proposed steps of the synthetic reaction.

Table 1 Volumetric titration of DAC for determination of average aldehyde content percentage (AC, %)

Vcontrol (ml)	Vsample (ml)	CNaOH (M)	m (gm)	AC %	Average AC%
0.5	2.7	0.1	0.1	35.2	35.71
0.5	2.7	0.1	0.1	35.2	
0.5	2.8	0.1	0.1	36.8	

Characterization

Infrared spectroscopy

The obtained IR spectra for native, DAC, DAC@Gu and DAC@GuTSC samples are presented in Fig. 2(a–d).

The FTIR spectrum of unmodified natural cellulose Fig. 2a and (Fig.S1a) shows some characteristic peaks in the range of 1000–1200 cm^{-1} corresponding to C-O elongation. While the peaks present at 1260–1410 cm − 1 are attributed to the OH bending vibrations, the peaks present between 3600 and 3200 cm^{-1} correspond to the OH stretching vibrations (Xu et al. 2013). Other peaks occurring at 2700–3000 cm^{-1} are due to C–H elongation.

The IR spectrum of DAC in Fig. 2.b and (Fig. S1b) shows an extremely sharp peak that is moderately sharp at about 1650 cm^{-1}, which is due to prolonged oscillations of the groups carbonyl (C=O) is formed during oxidation (Akl et al. 2021).

Modification of DAC by reaction with aminoguanidine causes some changes in the IR spectrum, notably a sharp peak at about 1720 cm^{-1}, possibly due to C=N formation between the aldehyde groups present in the cellulose being oxidants and amino groups of the added aminoguanidine [45] as shown in Fig. 2c and (Fig. S1c).

Figure 2d and (Fig. S1d) show the IR spectrum of DAC@GuTSC composite after insertion of phenyl isothiocyanate. The presence of new peaks between 1120 cm^{-1} and 960 cm^{-1} may be related to group C=S [49] present in the inserted phenyl isothiocyanate. Alternatively, the broad peak at about 2900 cm^{-1} could be due to the introduction of a phenyl group. Furthermore, the overlapping peaks occurring between 1520 cm^{-1} and 1650 cm^{-1} can be attributed to the unsaturated C–N–H, N=CH– and C=C bonds in the aromatic rings of the phenyl group (Balachandran and Murali 2011). The observed differences in IR spectra support the denaturation of natural cellulose and the insertion of new N and S functional groups into the newly prepared DAC@GuTSC composite.

Elemental analysis

The results of elemental analysis for native cellulose and modified cellulose are summarized in Table 2. The results revealed an addition of nitrogen and sulfur to the elemental composition of cellulose which indicates the successful

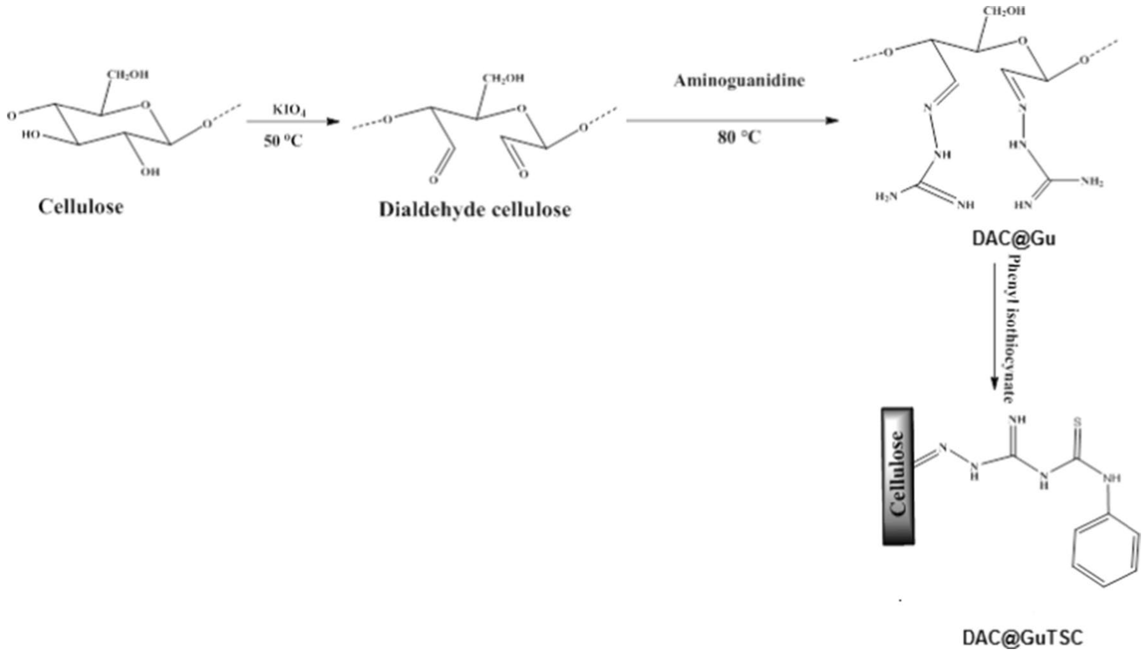

Scheme 2 Synthesis of DAC@GuTSC composite

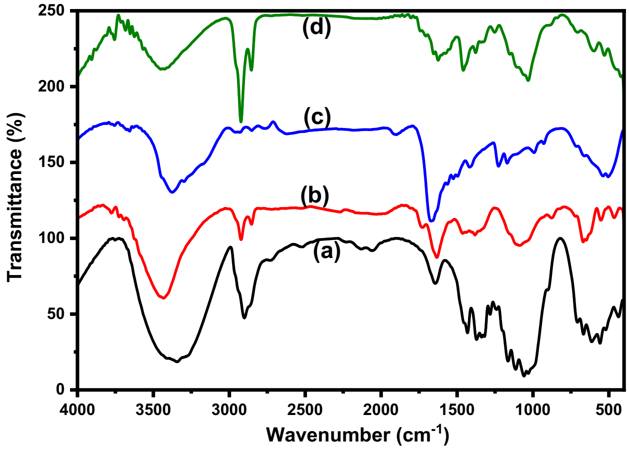

Fig. 2 FTIR of **a** native cellulose, **b** DAC, **c** DAC@Gu and **d** DAC@GuTSC composite

Table 2 Elemental analysis of native cellulose and DAC@GuTSC

Sample	Carbon (%)	Hydrogen (%)	Nitrogen (%)	Sulfur (%)
Native cellulose	44.5	7.14	–	–
DAC@GuTSC	46.4	5.81	8.32	3.81

modification of cellulose by introduction of new nitrogen and sulfur functional groups.

Scanning electron microscopy (SEM)

The surface morphology of DAC and DAC@GuTSC composite was studied by scanning electron microscopy at 5000X, 15000X and 27000X magnifications. Figure 3 shows the SEM images obtained at three magnifications. One can directly notice that the surface of the cellulose becomes rougher after being modified, which indicates the insertion of new moieties into the original structure. In addition, the surface of DAC@GuTSC has been shown to have large pores and pores that can help trapping metal ions during adsorption.

Brunauer–Emmett–Teller analysis (BET)

The BET surface analysis was applied to evaluate the specific surface properties of the samples. The results indicate that natural cellulose and the DAC@GuTSC sorbent are microporous materials in nature. In addition, BET-specific surface area calculations showed that natural cellulose fibers have a higher surface area (21.264 m^2 g^{-1}) than DAC@GuTSC composite (3.038 m^2 g^{-1}), Table 3. The decrease in surface area after chemical modification may be due to the covering of cellulose pores by anchoring guanyl thiosemicarbazide moieties which reduces the adsorption of N_2 molecules used in the surface measurement. The relatively low surface area of the functionalized fibers suggests that the adsorption occurs mainly through the coordination of the N, N- and N, S donors of the guanyl thiosemicarbazide moieties with metal ions.

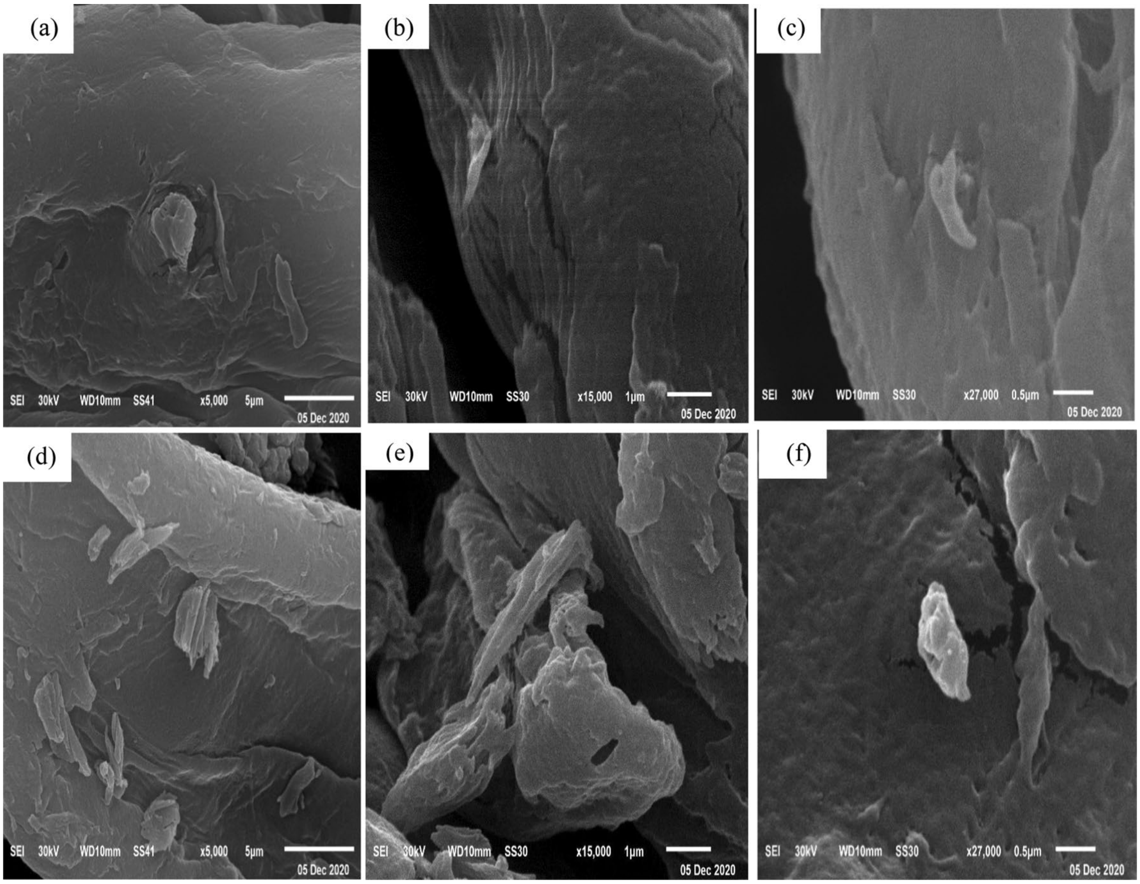

Fig. 3 SEM images of oxidized cellulose at **a** 5000×, **b** 15000×, **c** 27,000× and DAC@GuTSC at **d** 5000×, **b** 15,000× and **f** 27000×

Table 3 BET analysis results

Sample weight	Adsorptive	Adsorption temperature	Mean pore diameter (nm)	Surface area ($m^2 g^{-1}$)	Total pore volume ($cm^3 g^{-1}$)
0.0753	N2	77 K	4.7503	3.038	0.003608

Thermal gravimetric analysis (TGA)

A thermal gravimetric analysis (TGA) was performed to investigate the thermal decomposition of the DAC@GuTSC adsorbent before and after adsorption of heavy metal ions. As shown in Fig. 4, in the temperature range (0–200) °C, there is a very slight weight loss that actually starts after 100 °C mainly due to the evaporation of the water parts. The reduced mass started to increase from about 250 °C to about 450 °C due to the pyrolysis of the sample. Similar decomposition behavior was observed before and after adsorption. The heatmap of natural cellulose shows two stages of thermal degradation that typically yield levoglucosan and anhydrocellulose (Mohan et al. 2006). While the thermogram obtained from DAC@GuTSC composite in Fig. 4a shows four stages of thermal decomposition, which in turn confirms the appearance of a change in the composition of natural cellulose. At 750 °C, the final residual weight of DAC@GuTSC composite is 0.96%, indicating the remarkable thermal stability of DAC@GuTSC composite at very high temperatures. After adsorption of metal ions, the final remaining mass of the DAC@GuTSC–metal complex at 750 °C was 41.3%, 40.2% and 56.1% for DAC@, GuTSC-Cu, DAC@GuTSC-Hg and DAC@GuTSC-Pb, respectively. The increased residue value after metal adsorption compared with DAC@GuTSC composite indicates their higher thermal stability.

Adsorption studies

Point of zero charge (pH_{PZC})

The pH_{PZC} of adsorbent is one way to understand the absorption mechanism. The surface charge of the DAC@GuTSC adsorbent was assessed by measuring the pH_{PZC}. In general, adsorbents will show better affinity for anions at $pH < pH_{PZC}$ and vice versa. The pH_{PZC} value obtained for the DAC@GuTSC composite is about 5.75, Figure

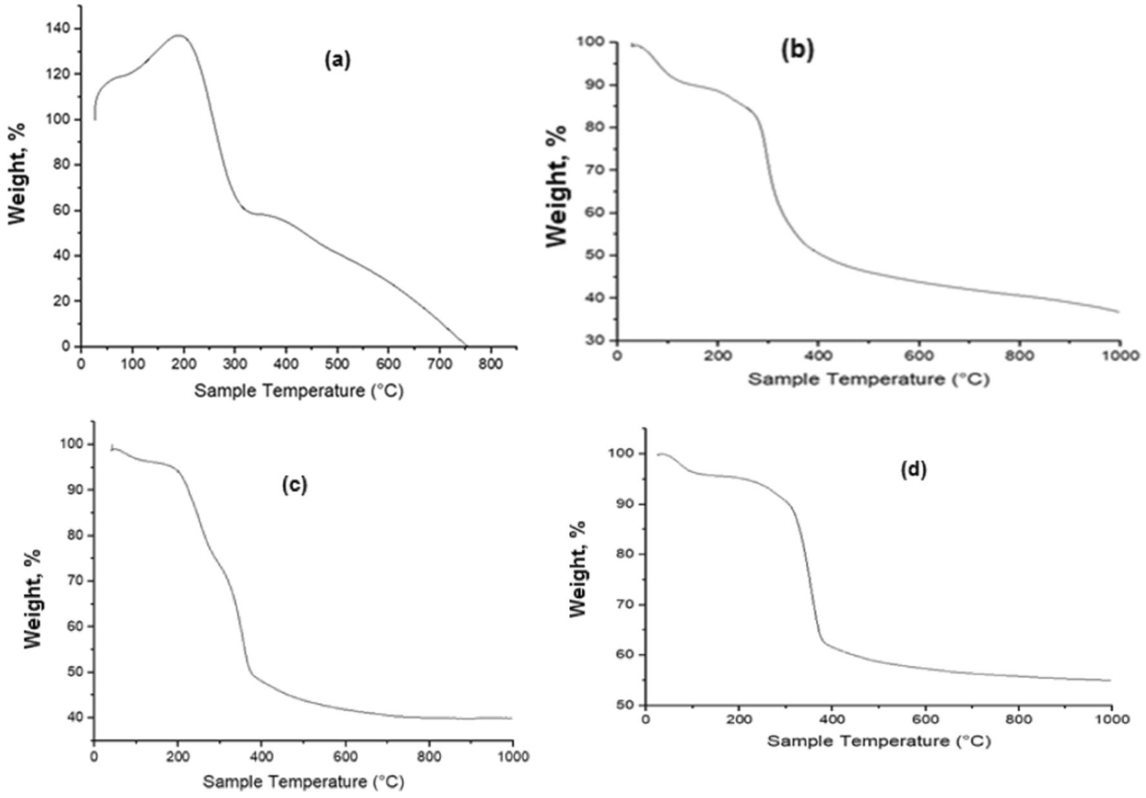

Fig. 4 TGA curves of **a** DAC@GuTSC, **b** DAC@GuTSC-Cu, **c** DAC@GuTSC-Hg, **d** DAC@GuTSC-Pb

S2. It is expected that the adsorption of metal ions can be increased at the experimental pH (pH = 6) by electrostatic interaction between Hg(II), Cu(II) and Pb(II), and the nitrogen-containing functional groups on the surface of DAC@GuTSC.

Effect of pH

The influence of pH value in the range 1.0–7.0 on metal removal by DAC@GuTSC is shown in Fig. 5. The adsorption capacity (qe) exhibits an increasing trend with increase in pH value until peaking at pH 6 for Cu^{2+}, Hg^{2+} and Pb^{2+}. The observed decrease trend in the removal % at low pH values can be explained by protonation taking place in an

Fig. 5 Effect of pH on the adsorption of Cu, Hg and Pb onto DAC@GuTSC composite

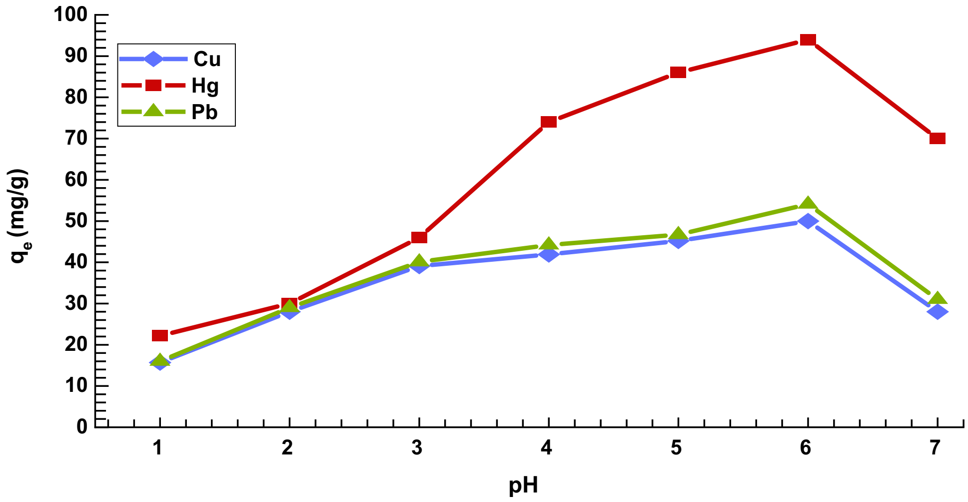

acidic environment where protons are attached to negatively charged groups on the fiber of the adsorbent, thereby competing with the intended metal ions to be adsorbed.

Effect of adsorbent dose

The adsorbent dosage was varied from 0.01 g to 0.1 g and the adsorption capacity was estimated for each dose. Figure 6 describes the relationship between adsorbent dosage and adsorption capacity of DAC@GuTSC adsorbent. From the figure, it can be concluded that the adsorption capacity increases as the adsorbent dose increases in a direct relationship, which may simply be due to the increased number of active sites. Then, when heavy metal saturation is reached, the adsorption capacity becomes constant as the adsorbent dosage increases. Cu^{2+} and Pb^{2+} show saturation values at 0.05 g of DAC@GuTSC adsorbent, while the maximum adsorption capacity for Hg^{+2} is only 0.03 g. The obtained results have proven that the DAC@GuTSC adsorbent is a very effective heavy metal adsorbent with very low dosage.

Effect of the initial metal ion's concentration and adsorption isotherms

The effect of the initial concentration (C_0) of different metal ions on the adsorption performance of DAC@GuTSC composite is shown in Fig. 7. All the metal ion adsorption curves of DAC@GuTSC composite have similar trends. As the initial concentration of metal ions in the solution increases, the adsorption capacities of DAC@GuTSC composite for various metal ions show an overall upward trend. After reaching a certain concentration, the upward trend of the adsorption curve slows down. An increase in the concentration of metal ions means that the absolute content of metal ions per unit volume increases. The chance of metal ions contacting DAC@GuTSC composite increases, resulting in a rapid increase in the amount of metal ions adsorbed. However, with a further increase in the initial concentration, the adsorption efficiency of DAC@GuTSC for metal ions reaches saturation, and the growth rate of the adsorption curve becomes flat.

To better represent the effect of initial concentration on adsorption, Langmuir and Freundlich's adsorption isotherm models were used using linearization Eqs. (4) and (5)

$$\ln q_e = \ln K_F + 1/n \ln C_e \tag{4}$$

$$C_e/q_e = \left(1/K_L q_m\right) + \left(C_e/q_m\right) \tag{5}$$

where q_e is the equilibrium adsorption capacity, K_F is the Freundlich constant, n is the heterogeneity coefficient reflecting the energy distribution in the bonds, C_e is the equilibrium metal concentration, K_L is the Langmuir constant, and q_m is the maximum adsorption capacity of a layer.

The adsorbent convenience was then investigated by calculating (R_L) as the constant of the separation coefficient using Eq. (6).

$$R_L = 1/\left(1 + C_o K_L\right) \tag{6}$$

where K_L is the Langmuir adsorption constant and C_o is the initial concentration of metal ions.

R_L values greater than 1.0 indicate adsorbent mismatch, while R_L values between 0 and 1 indicate adsorbent concordance. The derived parameters are listed in Table 4. From the estimated values of the parameters for DAC@GuTSC, it is found that the correlation coefficients in Langmuir's model are very high, which means the real data correspond

Fig. 6 Effect of adsorbent dose on the adsorption of Cu, Hg and Pb

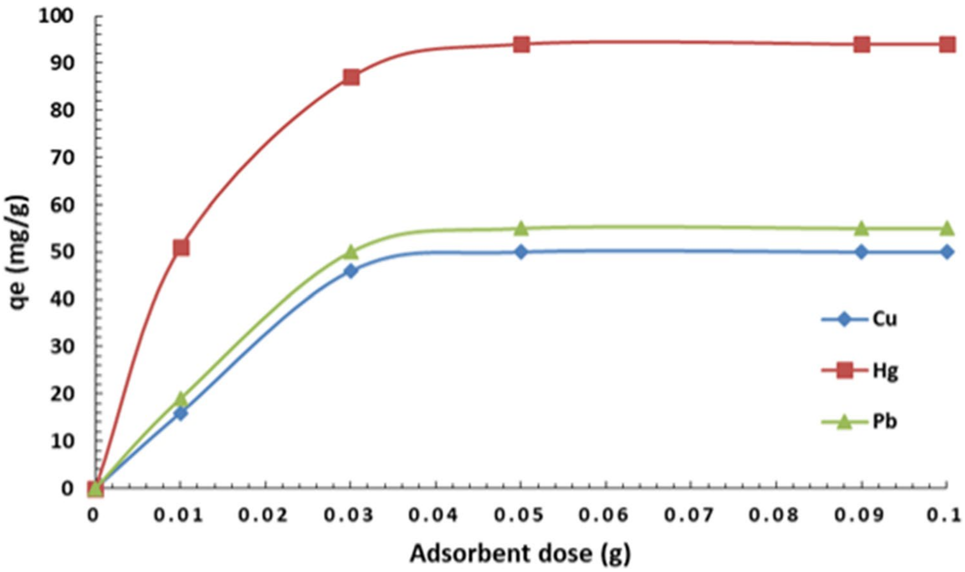

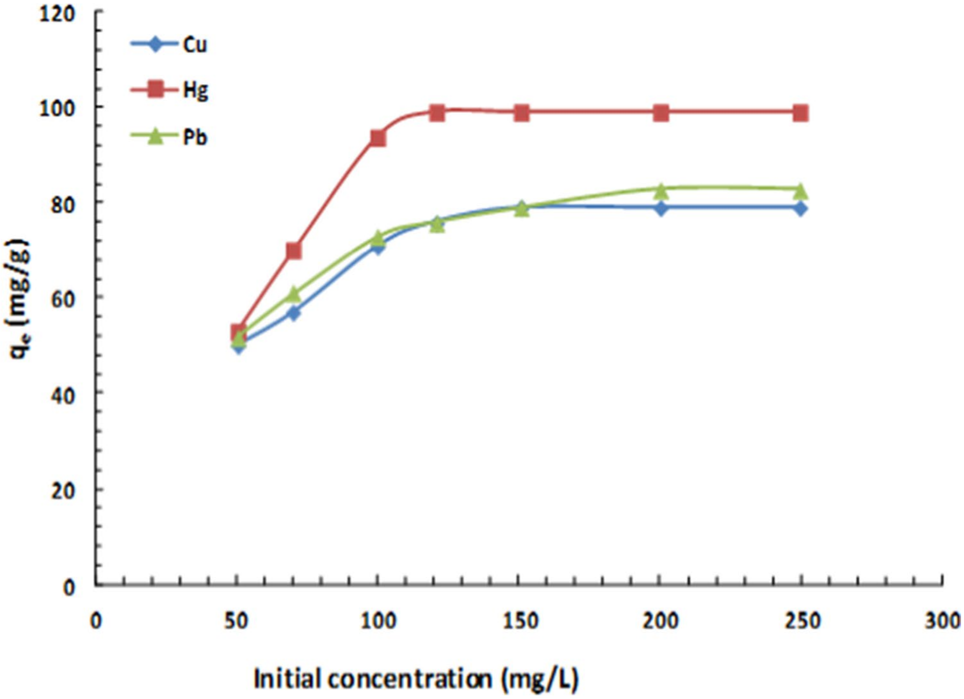

Fig. 7 Effect of initial metal ion concentration on the adsorption of Cu, Hg and Pb onto DAC@GuTSC

Table 4 Langmuir and Freundlich constants for metal adsorption by DAC@GuTSC

Langmuir isotherm model				
Adsorbates	K_L(L/g)	q_m (mg/g)	R_2	R_L
Cu^{2+}	0.384	80.65	0.9992	0.0103–0.0495
Hg^{2+}	12.625	99.01	1	0.0003–0.0017
Pb^{2+}	0.366	84.03	0.9993	0.0108–0.0518
Freundlich isotherm model				
Adsorbates	K_F	n	R_2	
Cu^{2+}	62.23	24.04	0.7721	
Hg^{2+}	82.02	21.23	0.8716	
Pb^{2+}	64.70	24.04	0.8479	

significantly to the model Langmuir. Meanwhile, the R^2 coefficients obtained from the Freundlich isotherm plot are much lower. In addition, the maximum adsorption capacity for one layer (q_m) obtained from the Langmuir plot is consistent with the experimental records, which clearly confirms that the adsorption process will be better described by Langmuir's isothermal model. All calculated values of R_L ranged from 0.0 to 1.0, confirming the suitability of DAC@GuTSC as adsorbent for the metal ions studied.

Effect oscillation time and adsorption kinetics

Figure 8 shows the effects of oscillation time on the adsorption of Cu^{2+}, Hg^{2+} and Pb^{2+} onto DAC@GuTSC. It can be seen that removal efficiency and adsorption capacity all increased rapidly and then remained stable with the increase in oscillation time. In adsorption initial stage, there were many usable adsorption sites in the surface DAC@GuTSC, accelerating the adsorption speed of Cu^{2+}, Hg^{2+} and Pb^{2+}. As time went on, a large number of empty adsorption sites had been occupied by Cu^{2+}, Hg^{2+} and Pb^{2+}. This leads to the reduction of effective adsorption sites and adsorption speed. Thus, in the later stage, their removal efficiency and adsorption capacity unchanged insignificantly and finally reached equilibrium. The selection of proper adsorption equilibrium time can effectively shorten adsorption period. Thus, the oscillation time for the adsorption of Cu^{2+}, Hg^{2+} and Pb^{2+} was 240 min.

Figure 8 represents the relationship between time of contact and adsorption capacity for DAC@GuTSC-Hg^{2+} by DAC@GuTSC composite was the most rapid followed by Pb^{2+} and Cu^{2+}. Maximum adsorption capacity of DAC@GuTSC composite was reached approximately in the first 6 h and then equilibrium was reached.

The obtained experimental data have been adapted to two kinetic adsorption models; pseudo-first and pseudo-second-order models to predict the adsorption mechanism. The kinematic parameters are calculated using Eqs. (7) and (8).

Fig. 8 Effect of oscillation time on the adsorption of Cu, Hg and Pb onto DAC@GuTSC

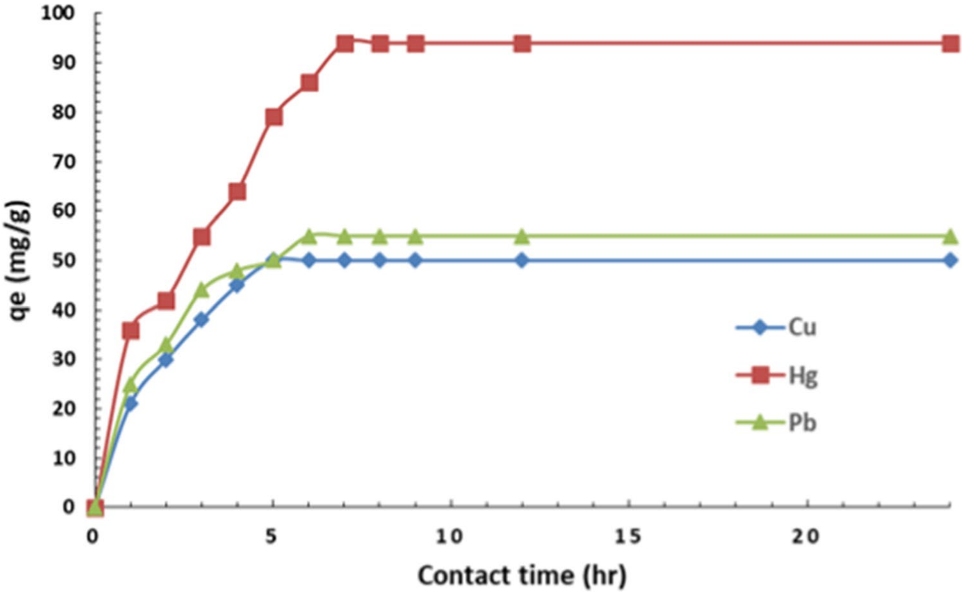

Pseudo-first-order (PFO) linear equation:

$$1/q_{t(\mathrm{ads})} = k_1/q_{e(\mathrm{ads})}t + 1/q_{e(\mathrm{ads})} \tag{7}$$

Pseudo-second-order (PSO) linear equation:

$$t/q_{t(\mathrm{ads})} = 1/k_2q^2_{e(\mathrm{ads})} + \left(1/q_{e(\mathrm{ads})}\right)t \tag{8}$$

where $q_{e(\mathrm{ads})}$ is the equilibrium adsorption capacity, $q_{t(\mathrm{ads})}$ is the adsorption capacity at time t, K_1 is the adsorption rate constant of the pseudo-first-order model, and K_2 is the adsorption rate constant.

The estimated kinetic parameters from the two models are summarized in Table 5, while the plotted curves are shown in Fig. 9. From the parameters obtained from the pseudo-first-order curves, it can be seen that the correlation coefficients (R^2) are high, but the theoretical equilibrium adsorption capacity $q_{e(\mathrm{ads})}$ for each metal does not match the experimental profile. On the other hand, the parameters calculated by pseudo-second-order model are consistent with the experimental results because the R^2 value is also high when approaching 1 and the adsorption capacity is consistent with the experimental results. Regarding the rate constants (K_1 and K_2) calculated in each model, it can be directly observed that the rate constants calculated from the first-order model are high, that is, the adsorption rate is slow, and therefore, it is inconsistent with the experimental results. Meanwhile, the rate constants obtained from the pseudo-second-order model are much smaller, which is more significant and correlated with experimental results. Thus, it can be deduced that the adsorption of Cu^{2+}, Hg^{2+} and Pb^{2+} by the DAC@GuTSC composite exhibits a pseudo-second-order kinetic model perfectly. It can also be concluded that chemisorption is the main dominant process and it is also believed to be the limiting factor.

Table 5 Kinetic parameters derived from pseudo-first-order model and pseudo-second-order model for adsorption of (Cu^{2+}, $Hg^{2+}$and Pb^{2+}) by DAC@GuTSC

	Cu^{2+}	Hg^{2+}	Pb^{2+}
Pseudo-first order			
$q_{e(\mathrm{ads})}$ (mg/g)	62.11	108.7	64.9
K_1 (min^{-1})	116.77	135.97	97.51
R^2	0.9712	0.9031	0.9709
Pseudo-second order			
$q_{e(\mathrm{ads})}$ (mg/g)	53	105.26	58
k_2 (g/(mg min)	3.9×10^{-4}	8.65×10^{-5}	3.47×10^{-4}
R^2	0.9943	0.9842	0.9959

Effect of temperature thermodynamic parameters

To investigate the effect of temperature on the adsorption of the studied metal ions, several thermodynamic properties were investigated, including the Gibbs free energy change ($\Delta G°$), the thermal equilibrium constant ($\underline{K}_c$), standard entropy change ($\Delta S°$) and standard enthalpy change ($\Delta H°$). The values of the mentioned thermodynamic parameters are calculated after plotting $1/T$ vs $\mathrm{LnK_c}$ using Eqs. 9–11.

$$K_C = C_{ad}/C_e \tag{9}$$

$$\ln K_C = \Delta S^{\mathrm{o}}_{\mathrm{ads}}/R - \Delta H^{\mathrm{o}}_{\mathrm{ads}}/RT \tag{10}$$

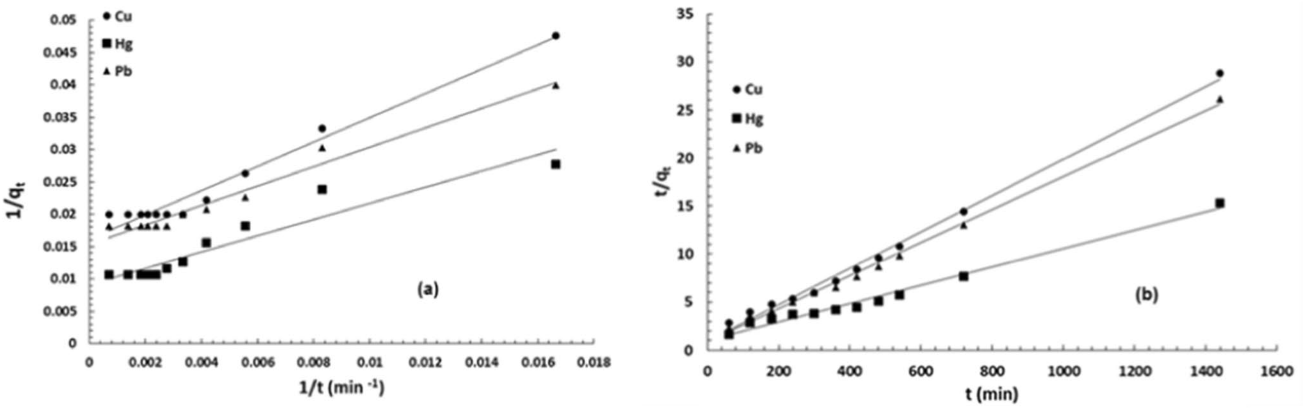

Fig. 9 Adsorption kinetics models: **a** PFO, **b** PSO models

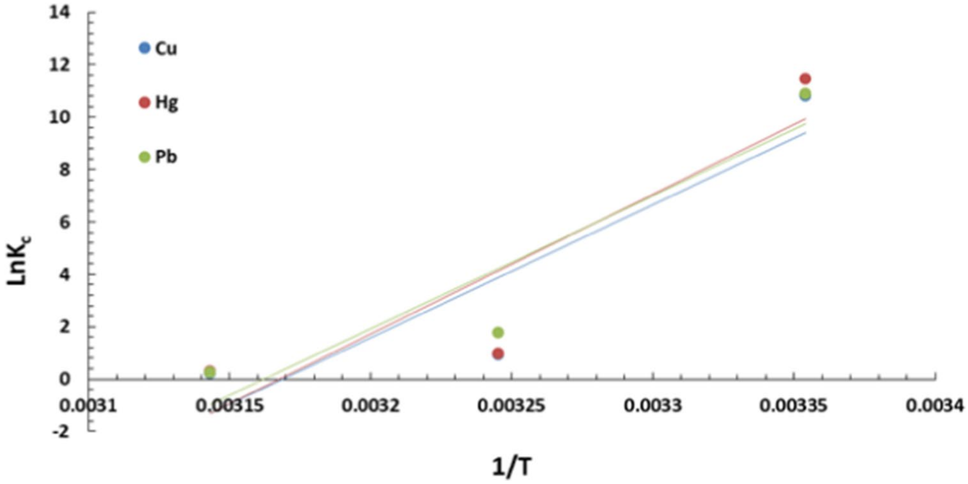

Fig. 10 Relation between Lnk$_c$ and 1/T for adsorption of Cu^{+2}, Hg^{+2} and Pb^{+2} onto DAC@GuTSC

R is gas constant (8.314 J/mol K).

$$\Delta G^{o}_{ads} = -RT\ln K_C \tag{11}$$

Figure 10 shows that the curves are plotted and the values obtained are all listed in Table 6. The temperature range studied is 298–318 K. The thermodynamic parameters of the adsorption of Cu^{+2}, Hg^{+2} and Pb^{+2} by DAC@GuTSC adsorbent are described in Table 6.

Gibbs (ΔG^{o}_{ads}) free energy values for the whole adsorption process show the spontaneity of the adsorption process in the studied temperature range. The enthalpy change values ($\Delta H°$) are also negative for all adsorption processes indicating their exothermic behavior. The standard entropy change ($\Delta S°$) is a measure of the randomness or distribution of energy in a system. The negative $\Delta S°$ values also indicate that the low randomness reflects the high affinity between the two modified cellulose (DAC@GuTSC) and the adsorbed metal ions, which is a very good indication of the adsorption efficiency. Thus, it can be concluded that high temperature is not favorable for the adsorption of metal ions of the studied adsorbent. Therefore, it is best to conduct adsorption experiments at moderately low temperatures such as 298 K which is normal room temperature.

Table 6 Thermodynamic parameters of adsorption of Cu^{+2}, Hg^{+2} and Pb^{+2} by DAC@GuTSC

	ΔG^{o}_{ads} (KJ /mol)			ΔH^{o}_{ads} (KJ/mol)	ΔS^{o}_{ads} (J/mol K)
	298 K	308 K	318 K	− 421.39	− 1335.15
Cu^{2+}	− 26.82	− 2.42	− 0.59		
Hg^{2+}	− 28.39	− 2.55	− 0.85	− 442.58	− 1401.82
Pb^{2+}	− 27.06	− 4.54	− 0.74	− 422.31	− 1335.48

Effect of some selected interfering ions:

The effect of the presence of foreign ions on heavy metal adsorption was investigated under optimal adsorption conditions. The percentage removal for each metal is estimated at 50 ppm for certain interfering ions. The concentration of the

Table 7 Removal of heavy metals on DAC@GuTSC in the presence of interfering ions

Interfering ions	Added concentrations of interfering ions (ppm)	% Removal		
		Cu^{2+}	Hg^{2+}	Pb^{2+}
Mg^{2+}	50	99.3	100	99.6
Fe^{2+}	50	98.7	98.4	98.1
Ca^{2+}	50	99.1	100	99.7
Al^{3+}	50	95.3	96.1	97.6
PO_4^{3-}	50	84.6	99.4	98.5
Acetate	50	98.2	98.7	97.6
Oxalate	50	98.3	98.6	99.1
Edetate	50	98.2	98.1	97.2

interfering ions is exactly equal to the metal concentration. All results are summarized in Table 7. From the results obtained, it can be concluded that the presence of 50 ppm cations such as Mg^{2+}, Fe^{2+}, Ca^{2+} and Al^{3+} and anions such as $PO_4{}^{3-}$, acetate, oxalate and edetate has no significant effect on heavy metal removal by DAC@GuTSC. The results give a promising indication of the selectivity of DAC@GuTSC, suggesting its potential for efficient operation in more complex media.

Effect of sample volume

In order to deal with real samples, especially water samples, containing very low concentrations of the metal ions, the maximum applicable sample volume must be determined. For this purpose, 25–1000 mL volumes of the model solutions containing 2–20 µg of the trace elements were passed through the column under the optimum conditions. The recovery values as a function of sample volume were quantitative and constant up to 1000 mL of the sample solution. The preconcentration factor was calculated as the ratio of the highest sample volume (1000 mL) to the eluent volume (10 mL) and found to be 100 for all the metal ions.

Desorption and reusability of DAC@GuTSC composite

To test the reusability of DAC@GuTSC, five cycles of adsorption–desorption have been carried out under the optimum conditions, using 5 ml of 0.5 M HNO_3, the obtained results are shown in Table 8. From the results, it was clear that the adsorption efficiency of DAC@GuTSC was only slightly decreased after cycle five, the adsorbent maintained about 95% of its initial efficiency.

Adsorption from multi-metal solutions

A mixture of metals under study was prepared to investigate the adsorption efficiency of the prepared DAC@GuTSC in multi-metal solutions. As shown in Table 9, the percentage removal shows the same trend of single-metal solutions without obvious difference. The results also correlate with the conclusion obtained in the ionic hindrance that DAC@GuTSC will perform efficiently in complex multi-component samples. The ICP OES is used to simultaneously determine the concentrations of multiple metal ions in the solutions studied.

Table 8 Repeated adsorption of metal ions Cu^{2+}, $Hg^{2+}$and Pb^{2+} (50 ml of 50 mg L L^{-1}) by DAC@GuTSC sorbent (0.050 g), pH 6, time of shaking 120 min, 25 oC, desorption by 5 mL of 0.5 mol/L HNO3

Cycle number	Recovery (%)		
	Cu^{2+}	Hg^{2+}	Pb^{2+}
1	99.4	99.6	99.1
2	98.5	98.6	98.1
3	97.7	97.2	97.3
4	96.4	96.3	96.8
5	95.6	95.2	95.6

Accuracy and application of the method

To study the accuracy of the proposed procedure, known amounts of analyte ions are added to tap water, Nile water and seawater samples, and then the proposed method is applied. The results are presented in Table 10. There is good agreement between the amount of metal added and the amount measured. The calculated recovery values are always greater than 95%, thus confirming the accuracy of the proposed procedure and its independence from matrix effects. These results confirm the validity of the proposed separation/pre-enrichment method.

Plausible mechanism of adsorption

To investigate the possible mechanism of metal ion adsorption onto DAC@GuTSC, the morphology, surface charge, optical images and FTIR of the adsorbent were evaluated.

Optical images Optical images of natural cellulose, oxidized cellulose (DAC), DAC@GuTSC and metal-loaded modified cellulose: DAC@GuTSC-Cu, DAC@GuTSC-Hg and DAC@GuTSC-Pb are shown in Fig. 11(a–f), respectively. The images show the obvious color change of the modified cellulose before metal absorption (light yellow) compared with the modified cellulose after metal absorption. These results indicate the tendency of DAC@GuTSC modified cellulose to adsorb investigated metal ions.

FTIR spectra of DAC@GuTSC before and after adsorption of metal ions The adsorption mechanism of the Cu, Hg and Pb metal ions was designed in light of the effective groups available on DAC@GuTSC surface as shown in Fig. 12a and

Table 9 Simultaneous removal of multi-metal solution of (Cu^{2+}, $Hg^{2+}$and Pb2 +) (50 ml of 50 mg L-1) by DAC@GuTSC sorbent (0.050 g), pH 6, time of shaking 120 min, 25 °C from natural water samples

Sample	Metal ion	Added (ppm)	Found[a] (ppm)	% Removal
Multi-metal solution of (Cu^{2+}, Hg^{2+} and Pb^{2+})	Cu^{2+}	50.0	5.25	89.5
	Hg^{2+}	50.0	8.4	91.6
	Pb^{2+}	50.0	4.59	90.82

[a] The concentration found in the aqueous solution after adsorption and ICP-AES determination

Table 10 Removal of single-metal solution of (Cu^{2+}, Hg^{2+} and Pb^{2+}) (50 ml of 50 mg L^{-1}) by DAC@GuTSC sorbent (0.050 g), pH 6, time of shaking 120 min, 25 °C from natural water samples (sample volume: 250 mL, final volume: 10 mL, n = 3)

Sample	Metal Ion	Added (μg)	Found (μg)	Recovery %
Tap water	Cu^{2+}	–	–	
		15.0	14.3	95.33
		30.0	29.2	97.33
	Hg^{2+}	–	–	
		15.0	14.5	96.67
		30.0	29.4	98,00
	Pb^{2+}	–		
		15.0	14.6	97.33
		30.0	29.5	98.33
Nile water	Cu^{2+}	–		
		15.0	14.4	96.00
		30.0	29.6	98.67
	Hg^{2+}	–		
		15.0	14.30	95.33
		30.0	29.4	98.00
	Pb^{2+}	–		
		15.0	14.4	96.00
		30.0	29.6	98.66
Sea water	Cu^{2+}	–		
		15.0	14.30	95.33
		30.0	29.2	97.33
	Hg^{2+}	–		
		15.0	14.5	96.67
		30.0	29.4	98,00
	Pb^{2+}	–		
		15.0	14.4	96.00
		30.0	29.2	97.33

(Fig. S3a). In fact, DAC@GuTSC composite is very abundant with active groups that can adsorb the three pollutants. These active groups come from the fact that the adsorbent is composed of dialdehyde cellulose and guanyl thiosemicarbazide which in their origin are rich in active groups.

FTIR spectrum of DAC@GuTSC–Cu(II), Fig. 12b and (Fig. S3b) was also used for evaluation of the mechanism by which the Cu^{2+}, as a representative example, can coordinate with the coordinating N,N donors and N,S donors present onto the DAC@GuTSC chelating fibers. The main characteristic peaks of azomethine presented obvious, shifted upon complexation with the Cu^{2+} ions. Thus, the value of stretching vibrations of C=N at 1610 $cm^{-1}$was moved to lower value at 1580 cm^{-1}, and this revealed that the complexation takes place between the two nitrogen atoms of the two C=N groups and copper ions. Moreover, coordination of thiolate S atom through –C–S–metal mode after enolization followed by deprotonation on sulfur to the metal ion is suggested by the shift of the ν(C=S) band at lower wave number in all of the studied complexes. The presence of a new band due to ν (M–S) at 420–425 cm^{-1} is another indication of the involvement of the S atom in coordination.

In conclusion, the DAC@GuTSC composite can bind to metal ions through N, N donors forming four- and five-membered chelate rings and through N, S donors forming six-membered chelate rings, Scheme 3

Performance of DAC@GuTSC

To increase the value of the sorbent, we conducted a comparative study of the maximum sorption capacity achieved for the same contaminants with other sorbents and activated carbon described in the literature. Table 11 summarizes different values of $q_{\max}$ for different sorbents. The adsorption of Cu, Hg and Pb observed in this study correlates with other studies with maximum adsorption capacities $q_{\max}$ for Cu, Hg and Pb at 298 K of 50, 94, and 55 mg g^{-1}. Comparing the adsorption capacities obtained from most of the studies mentioned, we found that the adsorption capacity of DAC@GuTSC is higher. Using Cu^{+2} as an example, DAC@GuTSC has an adsorption capacity of 50 mg g^{-1}, while all the methods described gave adsorption capacities ranging from 1.75 to 36 mg g^{-1}. Differences in Cu, Hg and Pb uptake are due to the morphological properties of each sorbent, including structure, functional groups and surface area. Desorption is an unavoidable process and an intermediate step for adsorbent regeneration. The latter is a key point for evaluating the reuse of sorbents for industrial applications due to environmental concerns and the need for sustainable development. In the future, experiments can be performed at column scale

Fig. 11 Optical images of **a** Native cellulose powder, **b** DAC oxidized cellulose, **c** DAC@GuTSC, **d** DAC@GuTSC-Cu, **e** DAC@GuTSC-Hg and **f** DAC@GuTSC-Pb

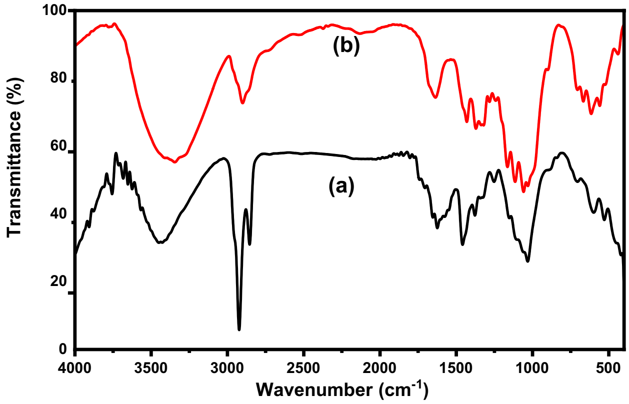

Fig. 12 FTIR of **a** DAC@GuTSC and **b** DAC@GuTSC-Cu(II)

and in pilot plants. These experiments can be implemented to be applied to sewage treatment plants to remove cationic and anionic metal ions and textile dyes from wastewater.

Conclusions

In order to find low-cost adsorbents, having pollutant-binding capacities is highly significant for efficient water treatment.

The results of the present study reveal that:

i. DAC@GuTSC composite may be highly applicable adsorbent for the removal of heavy metals from aqueous solutions.
ii. Modification of DAC by aminoguanidine and phenyl isothiocyanate significantly increased the nitrogen and sulfur-containing groups on the surface of DAC@GuTSC composite with remarkable change in textural properties and surface morphology.
iii. The adsorption of Cu^{2+}, Hg^{2+} and Pb^{2+} was dependent on initial concentration, reaction temperature and pH.
iv. The equilibrium of adsorption process could is well described by Langmuir adsorption isotherms, i.e., monolayer adsorption on a homogenous surface. The

Scheme 3 Plausible mechanism of Cu(II) onto DAC@GuTSC composite

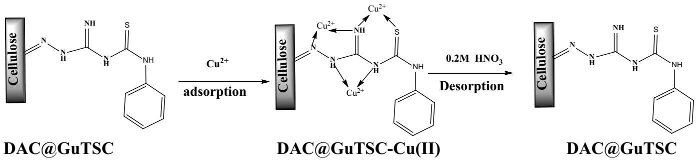

Table 11 Comparison of the adsorption capacities of Cu^{+2}, Hg^{+2} and Pb^{+2} by DAC@GuTSC with other adsorbents

Metal ion	Adsorbent	Adsorption capacity (mg g^{-1})	Reference
Cu^{+2}	DAC@GuTSC	50	Present work
	Microfibrillated cellulose modified with aminopropyltriethoxysilane	3.150	Hokkanen et al. (2014)
	Cellulose modified with acrylic acid	17.2	Güçlü et al. (2003)
	Cortex banana waste	36.0	Kelly-Vargas et al. (2012)
	Citric acid modified cellulose	24	Low et al. (2004)
	Pristine nanocellulose	20	Liu et al. (2015)
	Peanut shells	25.39	Witek-Krowiak et al. (2011)
	Orange peels modified with HNO_3 (0.1 M)	15.27	Lasheen et al. (2012)
	Cationic wheat straw	33.5	Zhong et al. (2014)
	Tobacco dust as a lignocellulosic source	36.0	Qi and Aldrich (2008)
	Pomegranate peel	30.12	Ben-Ali et al. (2017)
	Oil palm shell	1.75	Chong et al. (2013)
	Rice husk	30.0	Sobhanardakani et al. (2013)
Hg^{+2}	DAC@GuTSC	94	Present work
	Bamboo leaf powder as a cellulose source	27.11	Mondal et al. (2013)
	Guanyl modified cellulose	48	Khan et al. (2004)
	Eucalyptus bark	34.60	Ghodbane and Hamdaoui (2008)
	Bacillus subtilis biomass	68.5	Wang et al. (2010)
	Silica gel modified with 2-(2-oxoethyl)hydrazine carbothioamide	37.5 3	Chai et al. (2010)
	Allium sativum L	0.6497	Eom et al. (2011)
	Magnetic nanoparticles doped with 1,5-diphenylcarbazide	44	Zhai et al. (2010)
Pb^{+2}	DAC@GuTSC	55	Present work
	Cellulose powder modified with acrylic acid	55.9	Güçlü et al. (2003)
	Guanyl modified cellulose	52	Khan et al. (2004)
	Nano-TiO_2	7.41	Poursani et al. (2016)
	Citric acid modified cellulose	83	Mohan et al. (2006)
	Cotton as cellulosic biomass	10.78	Wu et al. (2012)
	Pine cone powder modified with NaOH(0.01 M)	24.75	Ofomaja and Naidoo (2010)
	Cauliflower waste	47.63	Hossain et al. (2014)
	Sorghum bicolor L. modified with thiourea	17.82	Ofomaja and Naidoo (2010)
	Oil palm shell	3.39	Chong et al. (2013)
	Tobacco dust as a lignocellulosic source	39.6	Qi and Aldrich (2008)
	S. bengalense extract modified with urea	12.65	Din et al. (2014)

kinetic studies follow a pseudo-second-order kinetic model.

v. The negative values of (ΔG^o) and (ΔH^o) thermodynamic parameters clarify the spontaneous and exothermic nature of the adsorption technique.

vi. In this study, the prepared DAC@GuTSC adsorbent has high removal efficiency of Cu^{2+}, Hg^{2+} and Pb^{2+} at optimum batch sorption condition with maximum sorption capacity of 50, 94 and 55 mg g^{-1} for Cu^{2+}, Hg^{2+} and Pb^{2+}, respectively, that was achieved within 240 min.

vii. The removal of Cu^{2+}, Hg^{2+} and Pb^{2+} from natural water samples was successfully applied using DAC@GuTSC.

viii. Submersion of the DAC@GuTSC-loaded metals samples in 5 ml of 0.5 M HNO_3 resulted in the desorption of more than 90% of the adsorbed metal ions.

ix. The uptake of Cu^{2+}, Hg^{2+} and Pb^{2+} using such DAC@GuTSC composite is highly comparable to the previous commercial adsorbents used for removal of Cu^{2+}, Hg^{2+} and Pb^{2+}.

x. The mechanism of adsorption was complex where DAC@GuTSC composite, possessing the synergistic effects of DAC and guanyl thiosemicarbazide, showed surface complexation between the **N, N-** and **N,** S donors of the guanyl thiosemicarbazide moiety with metal ions.

xi. In conclusion, the present work well demonstrated the potential of this technique for wider applications.

Supplementary Information The online version contains supplementary material available at https://doi.org/10.1007/s13201-023-01948-9.

Author contributions Magda A Akl was involved in conceptualization, supervision, investigation, methodology, visualization, writing—original draft, writing—review & editing. Abdelrahman S El-Zeny helped in writing—original draft, writing—review & editing. Mohamed Ismail contributed to supervision. Mohamed Abdalla was involved in supervision. Dina Abdelgelil helped in investigation, methodology, validation, visualization, writing—original draft, writing & editing. Aya G Mostafa contributed to investigation, methodology, writing—review & editing.

Funding Open access funding provided by The Science, Technology & Innovation Funding Authority (STDF) in cooperation with The Egyptian Knowledge Bank (EKB). This study received no support from public, private or nonprofit funding agencies.

Availability of data and materials Data supporting the results reported in the article can be requested from authors.

Declarations

Ethical approval The authors acknowledge that the current research has been conducted ethically. They declared that this manuscript does not involve researching about humans or animals.

Consent to participate The authors consent to participate in this research study.

Conflict of interest Authors declare no known competing interests.

Open Access This article is licensed under a Creative Commons Attribution 4.0 International License, which permits use, sharing, adaptation, distribution and reproduction in any medium or format, as long as you give appropriate credit to the original author(s) and the source, provide a link to the Creative Commons licence, and indicate if changes were made. The images or other third party material in this article are included in the article's Creative Commons licence, unless indicated otherwise in a credit line to the material. If material is not included in the article's Creative Commons licence and your intended use is not permitted by statutory regulation or exceeds the permitted use, you will need to obtain permission directly from the copyright holder. To view a copy of this licence, visit http://creativecommons.org/licenses/by/4.0/.

References

Acemioglu B, Alma MH (2001) Equilibrium studies on adsorption of Cu (II) from aqueous solution onto cellulose. J Colloid Interface Sci 243(1):81–84

Akl MAA, Kenawy IMM, Lasheen RR (2004) Organically modified silica gel and flame atomic absorption spectrometry: employment for separation and preconcentration of nine trace heavy metals for their determination in natural aqueous systems. Microchem J 78(2):143–156

Akl MAA-E, Kenawy IM, Lasheen RR (2005) Silica gel modified with N-(3-propyl)-o-phenylenediamine: Functionalization, metal sorption equilibrium studies and application to metal enrichment prior to determination by flame atomic absorption spectrometry. Anal Sci 21(8):923–931

Akl MA, Sarhan AA, Shoueir KR, Atta AM (2013) Application of crosslinked ionic poly (vinyl alcohol) nanogel as adsorbents for water treatment. J Dispersion Sci Technol 34(10):1399–1408

Akl MA, El-Zeny AS, Hashem MA, El-Gharkawy ESRH (2021) Synthesis, characterization and analytical applications of chemically modified cellulose for remediation of environmental pollutants. Egypt J Chem 64(7):3889–3901. https://doi.org/10.21608/ejchem.2021.65793.3412

Atta A, Akl MA, Youssef AM, Ibraheim MA (2013) Superparamagnetic core-shell polymeric nanocomposites for efficient removal of methylene blue from aqueous solutions. Adsorpt Sci Technol 31(5):397–419

Aydın H, Bulut Y, Yerlikaya Ç (2008) Removal of copper (II) from aqueous solution by adsorption onto low-cost adsorbents. J Environ Manage 87(1):37–45

Balachandran V, Murali MK (2011) FT-IR and FT-Raman spectral analysis of 3-(trifluromethyl) phenyl isothiocyanate. Elixir Vib Spec 40:5105–5107

Ben-Ali S, Jaouali I, Souissi-Najar S, Ouederni A (2017) Characterization and adsorption capacity of raw pomegranate peel biosorbent for copper removal. J Clean Prod 142:3809–3821

Bilal M, Shah JA, Ashfaq T, Gardazi SMH, Tahir AA, Pervez A, Haroon H, Mahmood Q (2013) Waste biomass adsorbents for copper removal from industrial wastewater—a review. J Hazard Mater 263:322–333

Chai X, Chang X, Hu Z, He Q, Tu Z, Li Z (2010) Solid phase extraction of trace Hg (II) on silica gel modified with 2-(2-oxoethyl) hydrazine carbothioamide and determination by ICP-AES. Talanta 82(5):1791–1796

Chang LW (1977) Neurotoxic effects of mercury—a review. Environ Res 14(3):329–373

Chaturvedi SI (2013) Electrocoagulation: a novel waste water treatment method. Int J Modern Eng Res 3(1):93–100

Chong HLH, Chia PS, Ahmad MN (2013) The adsorption of heavy metal by Bornean oil palm shell and its potential application as constructed wetland media. Biores Technol 130:181–186

Clarkson TW (1993) Mercury: major issues in environmental health. Environ Health Perspect 100:31–38

Clarkson TW, Magos L (2006) The toxicology of mercury and its chemical compounds. Crit Rev Toxicol 36(8):609–662

Dacrory S (2021) Antimicrobial activity, DFT calculations, and molecular docking of dialdehyde cellulose/graphene oxide film against Covid-19. J Polym Environ 29(7):2248–2260. https://doi.org/10.1007/s10924-020-02039-5

Dacrory S, Abou-Yousef H, Kamel S, Abou-Zeid RE, Abdel-Aziz MS, Elbadry M (2019) Functionalization and cross-linking of carboxymethyl cellulose in aqueous media. Cell Chem Technol 53(1–2):23–33

Din MI, Hussain Z, Mirza ML, Shah AT, Athar MM (2014) Adsorption optimization of lead (II) using Saccharum bengalense as a non-conventional low cost biosorbent: isotherm and thermodynamics modeling. Int J Phytorem 16(9):889–908

Dridi-Dhaouadi S, Douissa-Lazreg NB, M'Henni MF (2011) Removal of lead and Yellow 44 acid dye in single and binary component systems by raw Posidonia oceanica and the cellulose extracted from the raw biomass. Environ Technol 32(3):325–340

Eom Y, Won JH, Ryu J-Y, Lee TG (2011) Biosorption of mercury (II) ions from aqueous solution by garlic (Allium sativum L.) powder. Korean J Chem Eng 28:1439–1443

Friberg L, Mottet NK (1989) Accumulation of methylmercury and inorganic mercury in the brain. Biol Trace Elem Res 21:201–206

Gherasim C-V, Mikulášek P (2014) Influence of operating variables on the removal of heavy metal ions from aqueous solutions by nanofiltration. Desalination 343:67–74

Ghodbane I, Hamdaoui O (2008) Removal of mercury (II) from aqueous media using eucalyptus bark: kinetic and equilibrium studies. J Hazard Mater 160(2–3):301–309

Gotoh T, Matsushima K, Kikuchi K-I (2004a) Adsorption of Cu and Mn on covalently cross-linked alginate gel beads. Chemosphere 55(1):57–64

Gotoh T, Matsushima K, Kikuchi K-I (2004b) Preparation of alginate–chitosan hybrid gel beads and adsorption of divalent metal ions. Chemosphere 55(1):135–140

Güçlü G, Gürdağ G, Özgümüş S (2003) Competitive removal of heavy metal ions by cellulose graft copolymers. J Appl Polym Sci 90(8):2034–2039

Gupta VK (2009) Application of low-cost adsorbents for dye removal–a review. J Environ Manage 90(8):2313–2342

Guzzi G, La Porta CAM (2008) Molecular mechanisms triggered by mercury. Toxicology 244(1):1–12

Hokkanen S, Repo E, Suopajärvi T, Liimatainen H, Niinimaa J, Sillanpää M (2014) Adsorption of Ni (II), Cu (II) and Cd (II) from aqueous solutions by amino modified nanostructured microfibrillated cellulose. Cellulose 21:1471–1487

Hossain MA, Ngo HH, Guo WS, Nguyen TV, Vigneswaran S (2014) Performance of cabbage and cauliflower wastes for heavy metals removal. Desalin Water Treat 52(4–6):844–860

Hua M, Zhang S, Pan B, Zhang W, Lv L, Zhang Q (2012) Heavy metal removal from water/wastewater by nanosized metal oxides: a review. J Hazard Mater 211:317–331

Ibrahim A, El Fawal GF, Akl MA (2019) Methylene blue and crystal violet dyes removal (as A binary system) from aqueous solution using local soil clay: kinetics study and equilibrium isotherms. Egypt J Chem 62(3):541–554

Jamil N, Munawar MA, Muntaha ST (2009) Biosorption of Hg (II) and Cd (II) from waste water by using Zea Mays waste. J Chem Soc Pakistan 31

Kelly-Vargas K, Cerro-Lopez M, Reyna-Tellez S, Bandala ER, Sanchez-Salas JL (2012) Biosorption of heavy metals in polluted water, using different waste fruit cortex. Phys Chem Earth Parts a/b/c 37:26–29

Kenawy IM, Hafez MAH, Ismail MA, Hashem MA (2018) Adsorption of Cu(II), Cd(II), Hg(II), Pb(II) and Zn(II) from aqueous single metal solutions by guanyl-modified cellulose. Int J Biol Macromol 107:1538–1549. https://doi.org/10.1016/j.ijbiomac.2017.10.017

Khan NA, Ibrahim S, Subramaniam P (2004) Elimination of heavy metals from wastewater using agricultural wastes as adsorbents. Malaysian J Sci 23(1):43–51

Kurniawan TA, Chan GYS, Lo W-H, Babel S (2006) Physico–chemical treatment techniques for wastewater laden with heavy metals. Chem Eng J 118(1–2):83–98

Lasheen MR, Ammar NS, Ibrahim HS (2012) Adsorption/desorption of Cd (II), Cu (II) and Pb (II) using chemically modified orange peel: equilibrium and kinetic studies. Solid State Sci 14(2):202–210

Lee I-H, Kuan Y-C, Chern J-M (2007) Equilibrium and kinetics of heavy metal ion exchange. J Chin Inst Chem Eng, 38(1):71–84

Liu B, Huang Y (2011) Polyethyleneimine modified eggshell membrane as a novel biosorbent for adsorption and detoxification of Cr (VI) from water. J Mater Chem 21(43):17413–17418

Liu P, Borrell PF, Božič M, Kokol V, Oksman K, Mathew AP (2015) Nanocelluloses and their phosphorylated derivatives for selective adsorption of Ag+, Cu2+ and Fe3+ from industrial effluents. J Hazard Mater 294:177–185

Low KS, Lee CK, Mak SM (2004) Sorption of copper and lead by citric acid modified wood. Wood Sci Technol 38:629–640

Magos L, Clarkson TW (2006) Overview of the clinical toxicity of mercury. Ann Clin Biochem 43(4):257–268

Martin S, Griswold W (2009) Human health effects of heavy metals. Environ Sci Technol Briefs Citizens 15:1–6

Meena AK, Mishra GK, Rai PK, Rajagopal C, Nagar PN (2005) Removal of heavy metal ions from aqueous solutions using carbon aerogel as an adsorbent. J Hazard Mater 122(1–2):161–170. https://doi.org/10.1016/j.jhazmat.2005.03.024

Mohan D, Pittman CU Jr, Steele PH (2006) Pyrolysis of wood/biomass for bio-oil: a critical review. Energy Fuels 20(3):848–889

Mondal DK, Nandi BK, Purkait MK (2013) Removal of mercury (II) from aqueous solution using bamboo leaf powder: equilibrium, thermodynamic and kinetic studies. J Environ Chem Eng 1(4):891–898

Monier M, Akl MA, Ali W (2014a) Preparation and characterization of selective phenyl thiosemicarbazide modified Au(III) ion-imprinted cellulosic cotton fibers. J Appl Polym Sci 131(18):9277–9287. https://doi.org/10.1002/app.40769

Monier M, Akl MA, Ali WM (2014b) Modification and characterization of cellulose cotton fibers for fast extraction of some precious metal ions. Int J Biol Macromol 66:125–134

Navarro RR, Sumi K, Fujii N, Matsumura M (1996) Mercury removal from wastewater using porous cellulose carrier modified with polyethyleneimine. Water Res 30(10):2488–2494

Nayl AA, Abd-Elhamid AI, Abu-Saied MA, El-Shanshory AA, Soliman HMA, Akl MA, Aly HF (2020) A novel method for highly effective removal and determination of binary cationic dyes in aqueous media using a cotton–graphene oxide composite. RSC Adv 10(13):7791–7802

Nouri L, Ghodbane I, Hamdaoui O, Chiha M (2007) Batch sorption dynamics and equilibrium for the removal of cadmium ions from aqueous phase using wheat bran. J Hazard Mater 149(1):115–125

O'Connell DW, Birkinshaw C, O'Dwyer TF (2008) Heavy metal adsorbents prepared from the modification of cellulose: a review. Biores Technol 99(15):6709–6724

Ofomaja AE, Naidoo EB (2010) Biosorption of lead (II) onto pine cone powder: studies on biosorption performance and process design to minimize biosorbent mass. Carbohyd Polym 82(4):1031–1042

Pan B, Pan B, Zhang W, Lv L, Zhang Q, Zheng S (2009) Development of polymeric and polymer-based hybrid adsorbents for pollutants removal from waters. Chem Eng J 151(1–3):19–29

Poursani AS, Nilchi A, Hassani A, Shariat SM, Nouri J (2016) The synthesis of nano TiO 2 and its use for removal of lead ions from aqueous solution. J Water Resour Prot 8(04):438

Qi BC, Aldrich C (2008) Biosorption of heavy metals from aqueous solutions with tobacco dust. Biores Technol 99(13):5595–5601

Shoueir KR, Sarhan AA, Atta AM, Akl MA (2016) Macrogel and nanogel networks based on crosslinked poly (vinyl alcohol) for adsorption of methylene blue from aqua system. Environ Nanotechnol Monitor Manage 5:62–73

Shoueir KR, Atta AM, Sarhan AA, Akl MA (2017) Synthesis of monodisperse core shell PVA@ P (AMPS-co-NIPAm) nanogels structured for pre-concentration of Fe (III) ions. Environ Technol 38(8):967–978

Sobhanardakani S, Parvizimosaed H, Olyaie E (2013) Heavy metals removal from wastewaters using organic solid waste—rice husk. Environ Sci Pollut Res 20:5265–5271

Suhas, Gupta VK, Carrott PJM, Singh R, Chaudhary M, Kushwaha S (2016) Cellulose: a review as natural, modified and activated carbon adsorbent. Bioresour Technol 216:1066–1076. https://doi.org/10.1016/j.biortech.2016.05.106

Wang L, Li J (2013) Adsorption of CI Reactive Red 228 dye from aqueous solution by modified cellulose from flax shive: Kinetics, equilibrium, and thermodynamics. Ind Crops Prod 42:153–158

Wang XS, Li FY, He W, Miao HH (2010) Hg (II) removal from aqueous solutions by Bacillus subtilis biomass. Clean: Soil, Air, Water 38(1):44–48

Witek-Krowiak A, Szafran RG, Modelski S (2011) Biosorption of heavy metals from aqueous solutions onto peanut shell as a low-cost biosorbent. Desalination 265(1–3):126–134

Wu Z, Cheng Z, Ma W (2012) Adsorption of Pb (II) from glucose solution on thiol-functionalized cellulosic biomass. Biores Technol 104:807–809

Xu Y, Huang C, Wang X (2013) Characterization and controlled release aloe extract of collagen protein modified cotton fiber. Carbohyd Polym 92(2):982–988

Zewail TM, Yousef NS (2015) Kinetic study of heavy metal ions removal by ion exchange in batch conical air spouted bed. Alex Eng J 54(1):83–90

Zhai Y, Duan S, He Q, Yang X, Han Q (2010) Solid phase extraction and preconcentration of trace mercury(II) from aqueous solution using magnetic nanoparticles doped with 1,5-diphenylcarbazide. Microchim Acta 169(3):353–360. https://doi.org/10.1007/s00604-010-0363-8

Zhao G, Wu X, Tan X, Wang X (2010) Sorption of heavy metal ions from aqueous solutions: a review. Open Colloid Sci J 4(1)

Zhong QQ, Yue QY, Li Q, Gao BY, Xu X (2014) Removal of Cu(II) and Cr(VI) from wastewater by an amphoteric sorbent based on cellulose-rich biomass. Carbohyd Polym 111:788–796. https://doi.org/10.1016/j.carbpol.2014.05.043

Publisher's Note Springer Nature remains neutral with regard to jurisdictional claims in published maps and institutional affiliations.